Compact total irradiance monitor: Flight demonstration

Dave Harber*[a], Zach Castleman[a], Ginger Drake[a], Samuel Van Dreser[a], Nat Farber[a], Karl Heuerman[a], Joel Rutkowski[a], Alan Sims[a], Jacob Sprunck[a], Cameron Straatsma[a], Isaac Wanamaker[a], Wengang Zheng[a], Greg Kopp[a], Erik Richard[a], Peter Pilewskie[a,b], Nathan Tomlin[c], Michelle Stephens[c], Christopher Yung[c], Malcom White[c], John Lehman[c]

[a]Laboratory for Atmospheric and Space Physics, 1234 Innovation Drive, Boulder, CO, USA 80303-7814; [b]Dept. of Atmospheric and Oceanic Sciences, 4001 Discovery Drive, Boulder, CO USA 80309-0311; National Institute of Standards and Technology, 325 Broadway, Boulder, CO USA 80305-3337

ABSTRACT

The long-term balance between Earth's absorption of solar energy and emission of radiation to space is a fundamental climate measurement. Total solar irradiance (TSI) has been measured from space, uninterrupted, for the past 40 years via a series of instruments. The Compact Total Irradiance Monitor (CTIM) is a CubeSat instrument that will demonstrate next-generation technology for monitoring total solar irradiance. It includes novel silicon-substrate room temperature vertically aligned carbon nanotube (VACNT) bolometers. The CTIM, an eight-channel 6U CubeSat instrument, is being built for a target launch date in late 2020. The basic design is similar to the SORCE, TCTE and TSIS Total Irradiance Monitors (TIM). Like TSIS TIM, it will measure the total irradiance of the Sun with an uncertainty of <0.01% and a stability of <0.001%/year. The underlying technology, including the silicon substrate VACNT bolometers, has been demonstrated at the prototype-level. During 2019 we will build and test an engineering model of the detector subsystem. Following the testing of the engineering detector subsystem, we will build a flight detector unit and integrate it with a 6U CubeSat bus during late 2019 and 2020, in preparation for an on-orbit demonstration.

Keywords: solar irradiance, cubesat, carbon nanotubes, TSI

1. INTRODUCTION

The primary aspect of understanding Earth's climate change is understanding the rates and causes of climate variability both globally and regionally, which in turn requires distinguishing natural and anthropogenic causes. The Sun provides nearly all the energy powering the Earth's climate system. Measuring the total solar irradiance (TSI) with sufficient accuracy and long-term stability for discerning solar variability on multi-decadal timescales requires highly-accurate broadband radiometry and good long-term stability. This measurement has been performed from space by a 40-year uninterrupted sequence of instruments[1,2,3,4,5]. In order to maintain the long-term TSI record, these space-based measurements need to occur in perpetuity. It is then of great interest to use modern technological advances to develop miniaturized TSI instruments that can use CubeSat platforms to make these measurements.

The CubeSat platform provides a standardized size and interface for sizes from 1U (10×10×11 cm) to 27U (34×35×36 cm)[6,7,8]. These compact dimensions and the use of a standard set of sizes, mounting interfaces, and deployment has significantly reduced launch costs and increased launch opportunities. This has made small, low cost on-orbit technology demonstration missions possible. It also is opening the possibility of low-cost operational missions that rely on a constellation of independent satellites. Given the size limitations of CubeSats it is difficult to design in the redundancy and robustness possible in large platforms. However, multiple independent instruments with lower reliability replicate the reliability of a single high reliability instrument. For example, three independent instruments with a three year on-orbit survival probability of 63% yield a total three-year measurement success probability of 95%. Reducing the required reliability of a single CubeSat and instrument from 95% to 63% significantly reduces cost; this is most notable with electronic parts. Further, multiple instruments launched independently mitigate the risk of individual launch failures, such as the failed Glory-TIM TSI instrument launch in 2011. Given these factors, performing future TSI measurements with a small constellation of independent CubeSats would provide the low risk and cost-effective solution to the maintenance of the long-term TSI record.

*dave.harber@lasp.colorado.edu; phone 1 303 492-1387; fax 1 303 492-6444; lasp.colorado.edu

2. INSTRUMENT DESIGN

The Compact Total Irradiance Monitor (CTIM) is a miniaturized version of the SORCE, Glory, TCTE, and TSIS-1 Total Irradiance Monitor (TIM) [5] that will measure the total solar irradiance from a 6U CubeSat. The TIM detectors are cavity electrical substitution radiometers (ESR): closed-loop bolometers where the replacement heater power is adjusted to keep the bolometer temperature constant[9]. Incoming solar power is then detected by monitoring the replacement heater power as the incoming illumination, after passing through a precision aperture, is modulated with a shutter; typical shutter cycle times are 50 seconds open, 50 seconds closed. The four TIM bolometers are silver cavities 68 mm long and 16.5 mm in diameter at its entrance. The interiors of the cavities have coatings of etched nickel phosphorus (NiP) black and a replacement heater is wound onto the exterior of the cavity. These bolometers take approximately twelve months to fabricate and have a yield of only 15%.

The CTIM detectors are silicon-based vertically aligned carbon nanotube (VACNT) ESRs. Optical and thermal measurements of VACNTs have shown them to be nearly ideal optical absorbers; from the UV through the IR they are the best optical absorber known[10]. VACNTs exhibit good thermal conductivity along their length and display no degradation when exposed to ionizing radiation doses typical for low-earth orbit[11,12]. Additionally, microfabrication techniques allow the spatial extent of the VACNTs can be very precisely controlled. The use of a silicon substrate bolometer has several advantages. Silicon itself has good thermal diffusivity, only slightly lower than copper and aluminum and VACNTs can be patterned and grown directly onto silicon substrates. Additionally, silicon microfabrication allows for excellent control of the silicon in two dimensions and permits electrical traces to be patterned directly onto the silicon substrate. This allows most of the key elements of the bolometer to be fabricated onto a single piece of silicon. This combination of advantages makes silicon-VACNT bolometers promising for precise space-based radiometry in general, and measurement across the broad spectrum required for total solar irradiance in particular.
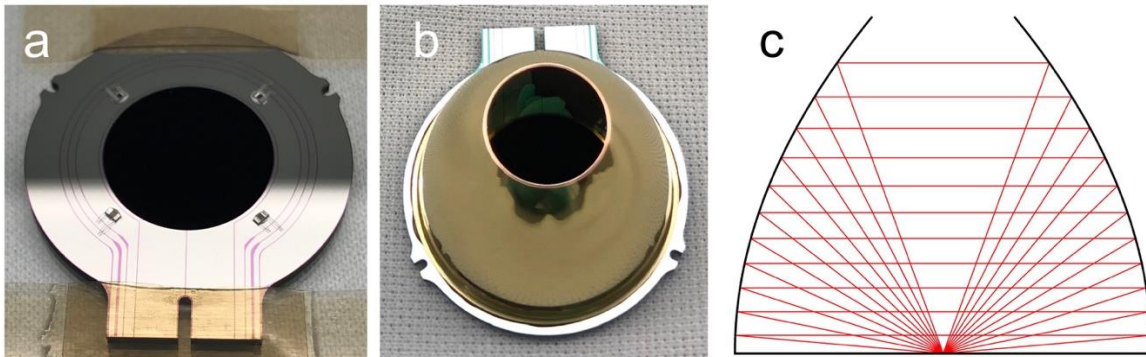
Figure 1: The CTIM silicon substrate detector (a). The detector with reflector dome attached (b). Ray trace of the reflector dome (c) showing that after two after two bounces light scattered by the VACNTs is redirected back.

The CTIM detectors, shown in Figure 1(a), are designed and fabricated by the NIST Sources and Detectors group. The VACNT absorber occupies then center 12 mm. Immediately outside is an annular tungsten heater. Four miniature thermistors are bonded directly to the silicon and connected electrically to conductive traces with wire bonds. In order to improve the optical absorption, and to reduce radiative coupling, an optical reflector is bonded directly onto the silicon substrate, Figure 1(b). This 51 µm thick reflecting dome increases optical absorption by more than a factor of ten and is thermally integrated with the substrate so that optical power absorbed by the reflecting dome is conducted into the silicon substrate, and so the reflecting dome itself is an optical absorber. Because of this, the reflectivity of the dome itself does not need to be individually characterized. Instead, the only reflectivity of the integrated bolometer plus dome needs to be measured, simplifying the detector characterization. In practice, because of the low reflectivity of the VACNTs and the high reflectivity of the reflecting dome, less than 0.05% of the incident light is absorbed by the reflecting dome itself.
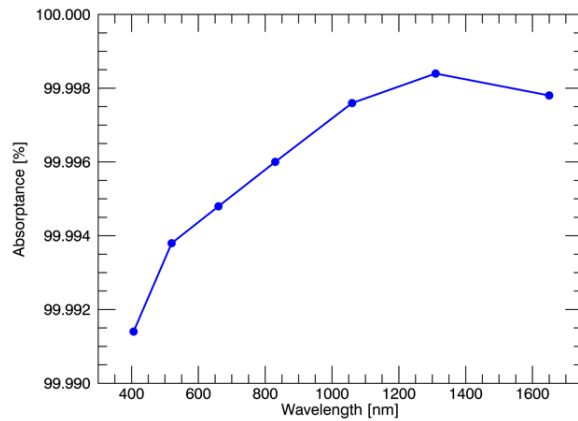
Figure 2: Measured absorptance across visible and near-infrared wavelengths for a typical CTIM detector.
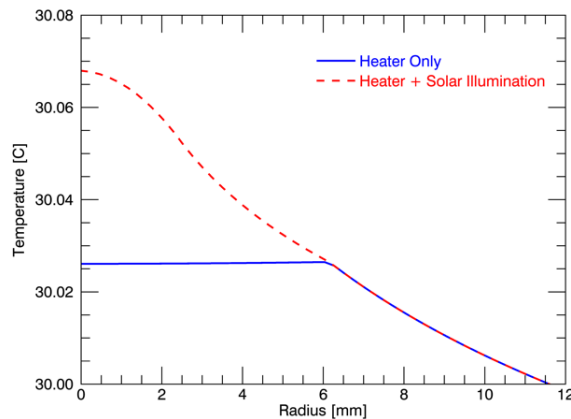
Figure 3: Modelled temperature distribution within the silicon substrate with heat power only (blue) or heater power plus the solar load (dashed red). The difference in the temperature distributions leads additional radiative loss for the solar illumination case and thus a non-equivalence between electrical and optical heating of 0.005%.

The shape of the reflecting dome is a parabola of rotation, with the focus at the center of the substrate. Light scattered from the VACNT absorber, which is nearly Lambertian, is redirected to the VACNTs after two reflections by the reflecting dome, Figure 1(c). A hemispherical reflector would accomplish the same with a single reflection, but the base width would be 64% greater, increasing the size of the entire instrument. With the reflecting dome, the absorptance of the detectors is greater than 99.99%, typical absorptance as a function of wavelength is plotted in Figure 2.

Thermal modelling of the detector was performed in order to determine the equivalence between electrical and optical heating; the results of thermal modelling of the detector is shown in Figure 3. The center of the detector is expected to be ~0.04 K greater during solar illumination than purely electrical heating resulting on an additional 0.005% of thermal emission and so a non-equivalence of 0.005%.

The detectors are mechanically mounted to the heat sink, a temperature-controlled aluminum block, with Kapton legs. These legs provide excellent thermal isolation; the detectors are primarily coupled to their surrounding environment by radiative coupling. The heat sink is temperature-controlled with a cold-biased heater, with CSIM 0.2˚ long-term stability was demonstrated with a similar control system. This level of thermal stability is important because thermal fluctuations of the heat sink can be seen in the detector, and so those fluctuations must be minimized at the measurement rate (60

seconds). In addition, there are secondary effects of thermal fluctuations, such as heater resistance and aperture area changes.
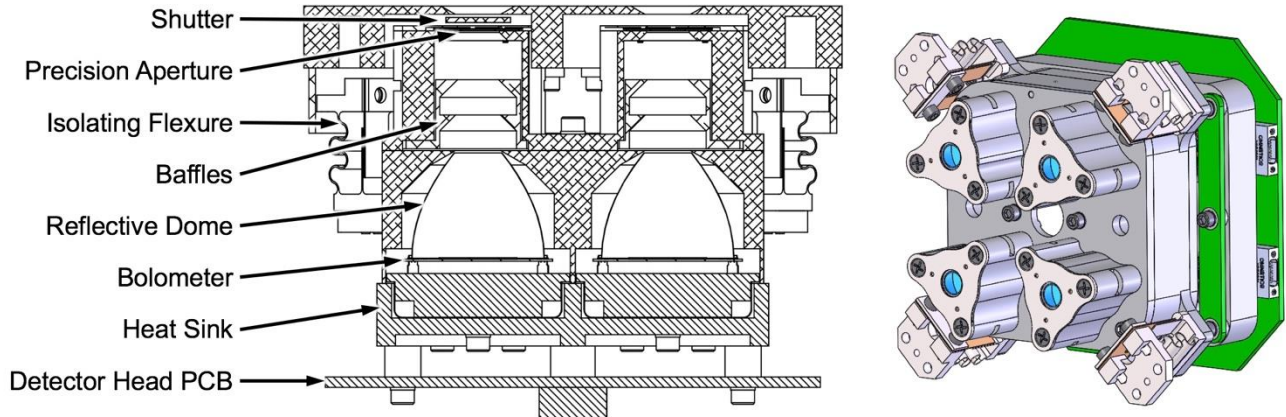
Figure 3: Cross-section of the CTIM detector head showing the optical design and key components (left). Model of the CTIM detector head showing the four channels and the detector head printed circuit board (PCB) in the back (right).

At the front of the instrument is a shutter, which is used to modulate the light with period of 60 seconds (30 seconds open, 30 seconds closed), see Fig. 3. Immediately following the shutter is a 5 mm diameter reactive ion-etched silicon aperture. These apertures, fabricated and measured at NIST, define the area of the irradiance measurement. Between the precision aperture and the detector assembly is a baffle section which reduces the sensitivity to off-axis light.

We are using a commercial off the shelf (COTS). These shutters, currently in operation on the CSIM-FD cubesat[13], have demonstrated >1 million cycle in laboratory life testing. In continuous operation with a 60 second cycle time there will be 525,960 cycles per year, and so we expect the primary channel shutter will operate for >1.9 years.

The detectors are electrically attached to the detector head printed circuit board (PCB) with wire bonds. The thermistor measurement and heater resistance tracking circuitry is on this PCB. The detectors are operated in pairs, with a Johnson noise-limited AC resistance bridge used to compare the resistance of the thermistors of an active detector against that from the reference detectors. The heater power to the active detector is adjusted so that the resistance of the active thermistor matches the resistance of the reference detector. We use this approach, rather than holding the resistance of the active detector to a fixed value, because cancels common-mode temperature drifts between the detector pair to first-order. The replacement heater power application and closed-loop control are essentially the same as those used in SORCE, Glory, TCTE, and TSIS TIM instruments[5].
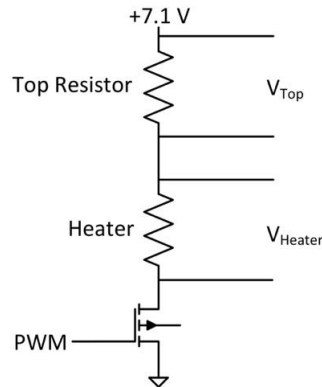
Figure 5: CTIM Bolometer heater configuration. The top resistor is equal in value to the heater. In situ heater resistance monitoring is implemented by turning on the pulse-width modulation (PWM) MOSFET on and then performing a measurement of the voltages V_{Top} and V_{Heater}.

One modification to the TIM heater power implementation[5] is the addition of a stabilizing series resistor along with the capability to monitor the heater resistance voltage in situ. The addition of the stabilization resistor, as shown in Figure 5, with a value equal to the heater resistance significantly decreases the sensitivity of the applied heater power to changes in the detector heater resistance; the temperature stability of the heater power is essentially determined by the temperature coefficient of this stabilization resistor. Moreover, by measuring the voltage drop across the heater resistor relative to the stabilization resistor we can monitor the ratio of their resistance. Thus, if we use a very stable top resistor, then we can both stabilize and monitor the detector heater resistance in situ. Commercial resistors with excellent long-term stability and very temperature coefficient of resistance (TCR) are readily available with typical TCRs of 0.2 ppm/°C and resistance drift of 1 ppm/year. This electrical configuration relaxes the stability and TCR requirements on the detector heater by about a factor of 100.

The heater voltage is provided a LTZ1000 voltage reference, as is used for the TIM instrument[5]. The LTZ1000 has been demonstrated to degrade 3.3 ppm/kRad[14]. The typical radiation dose rate for electrical components in a CubeSat in low earth orbit with 5mm of aluminum shielding is ~0.3 kRad/year, and so the expected drift of a is LTZ1000 on orbit due to radiation is 1 ppm/year; on the order of the long-term stability of the LTZ1000.

The detector head is mounted using four titanium flexures with integrated vibration damping provided by a layer of viscoelastic damping material. These flexures provide both thermal and mechanical isolation. The thermal isolation is needed to allow the detector head to be thermally stabilized with an actively controlled heater attached to the detector mounting block. The vibration isolation limits the launch loads on the detectors.

The TSI measurement uncertainty budget is detailed in Table 1, the expected total uncertainty is 0.0097%.

Table 1: TSI measurement uncertainty.

Correction	Value	Uncertainty
Aperture Area	100%	0.0022%
Diffraction Loss	0.042%	0.0042%
Detector Absorptance	0.010%	0.0020%
Heater Voltage	100%	0.0014%
Heater Resistance	100%	0.0028%
Heater Linearity	0.050%	0.0028%
Optical/Electrical Non-Equivalence	0.005%	0.0050%
Dark Signal	1.222%	0.0050%
	Total	*0.0097%*

3. CTIM FD IMPLEMENTATION

The CTIM CubeSat will accommodate two independent detector heads for a total of eight channels. Three to four channels are typically used in science operations of TSI sensors, CTIM will have two detector heads for a total of eight channels. The dual detector heads, each with four channels, will allow us to run at least two channels as primary channels, which receive the maximum solar exposure. By doing so we can improve statistics on degradation of the detectors with solar exposure. The remaining three channels on each detector head will be operated briefly daily, weekly and monthly. The ratio of exposure time between these channels will enable the solar-exposure related degradation of the bolometers to be determined and corrected[5].

Each detector is connected directly to the detector head PCB mounted directly to the detector head. The detector head PCB connects in turn to second PCB, the pulse-width modulation board. This board contains the LTZ1000 precision voltage references and the PWM MOSFETs and their associated circuitry. There are four PCBs that control the CTIM instrument: a FPGA based controller board, an ADC board with the science ADCs and DACs, and a board with power

conditioning, shutter control, heater control electronics, and the RS-422 communications interface with the CubeSat command and data handling (C&DH) electronics.
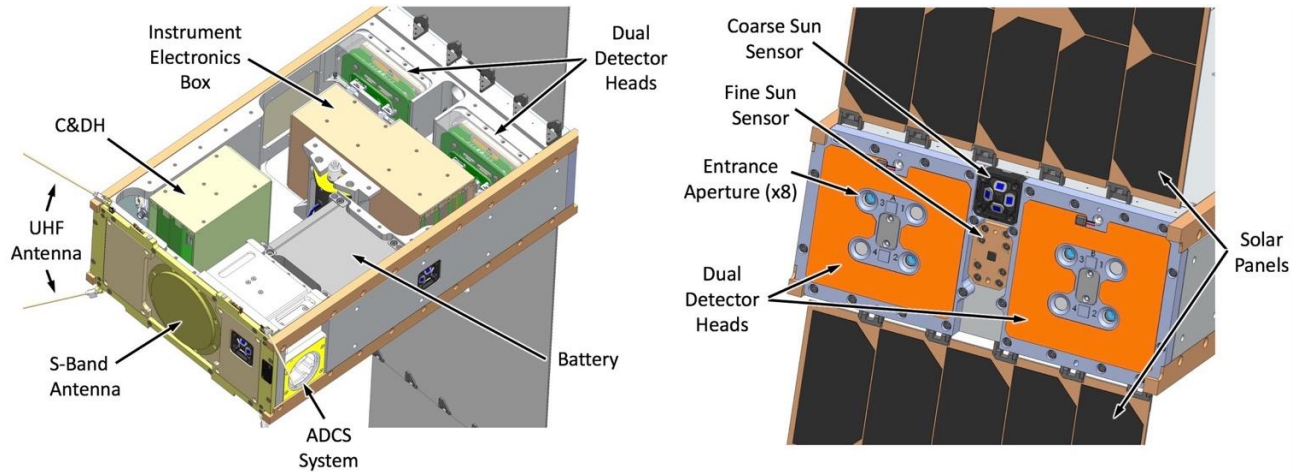
Figure 6: Layout of the 6U CTIM CubeSat.

The key CTIM CubeSat subsystems are summarized in Table 2. The CTIM CubeSat design is based upon the CSIM CubeSat[13] with design changes implemented to address lessons learned during the integration and test, and the early operations of the CSIM CubeSat.

Table 2: Summary of CTIM CubeSat components.

Component	Description
Command and Data Handling	Radiation tolerant FPGA + embedded processor design
Electrical Power System	4x6U panels, 75W total, with active deployment Dual 80 W-Hr battery packs Step-down battery charger
ACDS	Star tracker, 3x reaction wheels, 3x torque rods
S-Band Antenna	Patch antenna, non-deployable
UHF Antenna	Near-monopole, with active deployable

The most-significant technical constraint levied on the CubeSat design from the CTIM instrument is thermal stability of the detector heads. The thermal design accomplishes this by thermally isolating the detector heads via the titanium flexures and with four closed-loop controlled heaters. There are two heaters on the solar-facing surface of the CubeSat, one in front of each detector head. There is also a heater integrated into the base of each detector head. This will allow the detector head and the key thermal interface to be held at a constant temperature throughout the orbit. Finally, the power system is designed with a total of 160 W-hr of battery capacity and 75 W of solar array power to provide sufficient capacity so that the operation heaters can continuously, during sunlight and eclipse periods.

Table 3: Mission summary.

Correction	Value
TSI Measurement Uncertainty	0.0097%
TSI Measurement Long-Term Stability	<0.0001%/year
TSI Reporting Frequency	Every 6 hours
Orbital Altitude	450-600 km
Orbital Inclination	40°-60°
Payload	6U CubeSat
Mass	10 kg
Instrument Power Total Power	15 W 55 W
Communications: UHF (uplink) UHF (downlink) S-Band (downlink)	 9.6 kbps 9.6 kbps 1.0 Mbps
ADCS (3 axis)	10 arc-secs
Data Volume: UHF S-Band	 0.5 MB/day 37 MB/day
UHF UL Time UHF DL Time S-Band DL Time	>3 mins/day >6 mins/day >6 mins/day
Mission Life	1.0 Years

4. LAUNCH AND OPERATIONS

The integration and testing of the CTIM instrument and CubeSat will occur in 2020. Following completion of the spacecraft testing we will deliver CTIM to the launch provider and for installation into the CubeSat deployer. In order to ensure a mission life of at least a year the target orbit altitude for CTIM is 450 km or higher. In order to avoid the additional radiation associated with a polar orbit our target orbital inclination is between 40° and 60°; a 40° orbital inclination is needed in order for ground-passes over our ground station at LASP in Boulder, Colorado.

The CTIM mission will be operated from LASP using our existing UHF and S-Band ground stations. We plan on a one-year mission life, with the possibility for continued operations. The primary channel of each detector head will be cycled continuously with a period of 60 seconds (30 seconds shutter open, 30 seconds shutter closed), with the exception of when the channel is facing RAM. The measurements taken when facing the sun are obviously the measurements of the solar irradiance. In addition, measurements must be taken with the same channel facing deep space. This measures the dark signal of the channel, which is the amount of thermal radiation that the bolometer is emitting to deep space. This dark signal is subtracted from the measurements taken in the light in order to get an accurate measurement of solar irradiance.

Since each detector head consists of four bolometers, we have three channels in addition to the primary, or first, channel. These redundant channels are used to track the degradation experienced by the primary channel. The instrument configuration allows us to make measurements with these redundant channels concurrently with the primary channel. This is important because the solar variability over a day can be on the order of the differences between the channels. The second channel will be operated for one orbit per week, and the third and fourth channels operated with further reduced frequency. By comparing the ratios of the measurements taken by these channels we can develop a model of the degradation induced by solar exposure for these bolometers to correct for the degradation of the primary channel.

There are four key periods to the CTIM mission. First, is the commissioning, lasting approximately one month. During commissioning we will establish communications, ensure deployment of the solar panels and UHF antenna (the CTIM CubeSat can operate with both un-deployed), and functionally check out all CubeSat subsystems. Second is first light, where all CTIM channels will perform the first on-orbit TSI measurements. The first assessment of the CTIM uncertainty will be by comparing the inter-channel agreement four all eight CTIM channels, and by comparing to the current TSI level from TSIS-TIM. Finally, the third phase of operations is the normal operations. During this phase the primary channels of both detector heads will continuously cycle measuring, with the additional channels operating at their specified lower cadences. The time-series measurements of the two primary channels can be inter-compared and compared directly against the time series from TSIS-TIM. First of interest is the instrument performance over the short-term, for example over one solar rotation of ~27 days. Finally, after a timescale of several months to one year will an assessment to be made of the long-term stability of CTIM to be made relative to TSIS-TIM, providing the most stringent test of the long-term stability of the CTIM instrument.

ACKNOWLEDGEMENTS

REFERENCES

[1] Lee, R. B.III, M. A. Gibson, R. S. Wilson, and S. Thomas (1995), Long-term total solar irradiance variability during sunspot cycle 22, J. Geophys. Res., 100, 1667–1675, doi:10.1029/94JA02897.

[2] Fröhlich, C., and J. Lean (2004), Solar radiative output and its variability: Evidence and Mechanisms, Astron. Astrophys. Rev., 12(4), 273–320, doi:10.1007/s00159-004-0024-1.

[3] Fröhlich, C. (2009), Evidence of a long-term trend in total solar irradiance, Astron. Astrophys., 501, L27–L30, doi:10.1051/0004-6361/200912318.

[4] Willson, R. C., and A. V. Mordvinov (2003), Secular total solar irradiance trend during solar cycles 21–23, Geophys. Res. Lett., 30(5), 1199, doi:10.1029/2002GL016038.

[5] Kopp, G., and G. Lawrence (2005), The Total Irradiance Monitor (TIM): Instrument design, Sol. Phys., 230, 1–2, doi:10.1007/s11207-005-7446-4.

[6] Shiroma, W.A., Martin, L.K., Akagi, J.M. et al. cent.eur.j.eng (2011) 1: 9. https://doi.org/10.2478/s13531-011-0007-8

[7] Daniel Selva, David Krejci, A survey and assessment of the capabilities of Cubesats for Earth observation, Acta Astronautica, Volume 74, 2012, Pages 50-68, ISSN 0094-5765, https://doi.org/10.1016/j.actaastro.2011.12.014.

[8] Armen Poghosyan, Alessandro Golkar, CubeSat evolution: Analyzing CubeSat capabilities for conducting science missions, Progress in Aerospace Sciences, Volume 88, 2017, Pages 59-83, ISSN 0376-0421, https://doi.org/10.1016/j.paerosci.2016.11.002.

[9] F. Hengstberger, Absolute Radiometry, Academic Press, San Diego (1989), ISBN 0-12-340810-5

[10] Lehman et al. Appl. Phys. Rev. 5, 011103 (2018)

[11] H. Le Khanh et al., "Thermal interfaces based on vertically aligned carbon nanotubes : An analysis of the different contributions to the overall thermal resistance," 2010 16th International Workshop on Thermal Investigations of ICs and Systems (THERMINIC), Barcelona, 2010, pp. 1-4.

[12] J. Kuhnhenn, G. Lubkowski, Proton radiation effects on the optical properties of vertically aligned carbon nanotubes, Proc. of SPIE Vol. 10564 1056427-4

[13] E.C. Richard, D.M. Harber, G. Drake, Z. Castleman, J. Rutkowsi, M. Fowle, M. Miller, M. Fisher, A. Sims, J. Sprunck, P. Smith, M. Chambliss, W. Zheng, T. Woods, P. Pilewskie, N. Tomlin, M. Stephens, C. Yung, M. White, J. Lehman, "The compact spectral irradiance monitor: Flight demonstration mission," Proc. SPIE [##], Optical Engineering and Applications: CubeSat and NanoSat Instruments and Concepts II, ## (11 Aug 2019). In press.

[14] B. G. Rax, C. I. Lee and A. H. Johnston, "Degradation of precision reference devices in space environments," in IEEE Transactions on Nuclear Science, vol. 44, no. 6, pp. 1939-1944, Dec. 1997.